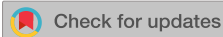


RESEARCH ARTICLE | FEBRUARY 01 1991

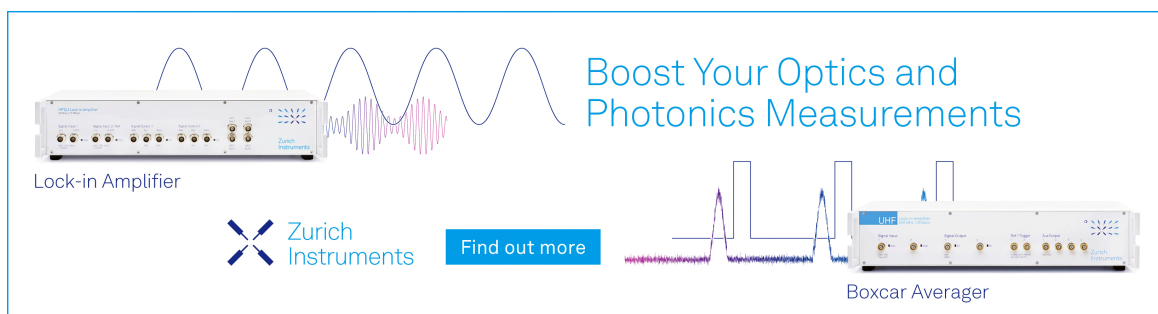
Relaxation dynamics in molecular alloys. I. Annealed $(\text{C}_2\text{F}_6)_{1-x}(\text{CClF}_3)_x$ mixtures

R. Böhmer; A. Loidl




J. Chem. Phys. 94, 2143–2148 (1991)

<https://doi.org/10.1063/1.459885>



Boost Your Optics and Photonics Measurements

Lock-in Amplifier

 Zurich Instruments

[Find out more](#)

Boxcar Averager

Relaxation dynamics in molecular alloys. I. Annealed $(\text{C}_2\text{F}_6)_{1-x}(\text{CClF}_3)_x$ mixtures

R. Böhmer^{a)} and A. Loidl

Institut für Physik, Johannes Gutenberg-Universität Mainz, D-6500 Mainz, Federal Republic of Germany

(Received 2 April 1990; accepted 18 October 1990)

Solid solutions of $(\text{C}_2\text{F}_6)_{1-x}(\text{CClF}_3)_x$ were investigated using dielectric spectroscopy. In part I of this work results on thermally equilibrated $(\text{C}_2\text{F}_6)_{1-x}(\text{CClF}_3)_x$ alloys are presented. The molar polarizability of liquid and plastic C_2F_6 was determined. The phase diagram of $(\text{C}_2\text{F}_6)_{1-x}(\text{CClF}_3)_x$ was studied in detail. It exhibits two eutectic points and a large miscibility gap. In a high-temperature orientationally disordered phase mixed crystals can be grown up to CClF_3 concentrations $x \approx 0.5$; in the low-temperature ordered state solid solutions are stable for $x < 0.25$. The dielectric loss spectra indicate that in $(\text{C}_2\text{F}_6)_{1-x}(\text{CClF}_3)_x$ different relaxation channels are available for the CClF_3 dipoles.

I. INTRODUCTION

Alloys composed of polar and nonpolar molecules are ideally suited to study the effects of molecular interactions on the dielectric response: at low dipolar defect concentrations the relaxation of isolated dipoles in a crystalline host matrix yields information about the local environment of the probes. With increasing dopant concentration, two effects have to be taken into account: (i) dipole-dipole interactions become important and (ii) the perturbation of the anisotropy of the host lattice strongly increases. In the latter case, different relaxation channels are accessible to the dipoles at different lattice sites. Finally, for large concentrations, the dipolar interactions will lead to long-range electric order.

At intermediate concentrations, molecular alloys can exhibit new ground states: site disorder and the anisotropic dipolar interactions can yield an orientational glass state at low temperatures.¹ This frozen-in disordered state seems to be a molecular analog to the spin glass state in dilute magnetic systems.² Glassy low temperature states can also be obtained by rapid cooling of the orientationally disordered high temperature phases. Supercooled $(\text{C}_2\text{F}_6)_{1-x}(\text{CClF}_3)_x$ crystals belong to this class of glassy crystals. This will be demonstrated in a succeeding paper.³ Here we present the results of our dielectric measurements on slowly cooled (i.e., thermally equilibrated) $(\text{C}_2\text{F}_6)_{1-x}(\text{CClF}_3)_x$ mixtures.

The C_2X_6 molecules where X is a halogen atom, form a series of solids with similar physical properties.⁴ Like C_2Cl_6 and C_2Br_6 , condensed C_2F_6 exhibits an orientationally disordered phase (β - C_2F_6)⁵ just below the melting point $T_m = 173$ K.^{5,6} In this β phase the C-C molecular axes are disordered.⁷ At $T = 104$ K the disorder is partially removed.⁵ This was concluded from anomalies in the specific heat^{5,8} and in the NMR linewidth.⁷ The structure of the β phase is unknown. Spectroscopic and x-ray investigations revealed a monoclinic low temperature (α -) phase.⁹

CClF_3 condenses at $T_m = 84.5$ K. Recently it has been

shown by neutron powder diffraction that below the melting point CClF_3 is antiferroelectrically ordered within an orthorhombic unit cell.¹⁰ There are no indications that structural phase transitions take place in this solid.^{11,12} However, dielectric measurements have revealed that near the melting point, this molecular crystal is close to a transition into a plastic phase.¹² This was indicated by the dielectric relaxation that could be detected in the solid.¹³ At low temperatures, the dynamics of CClF_3 were described in terms of thermally activated processes with an unusual low energy barrier of the order of 100 K. Additional relaxation mechanisms were seen to be active as an asymmetric broadening of the dielectric loss spectra close to the melting point.¹³ These high temperature reorientations were investigated recently using nuclear magnetic resonance experiments.¹⁴

This paper is organized as follows: In the next section the results of our dielectric investigation of C_2F_6 are given, forming the basis for the presentation of the measurements on mixtures with the dipolar compound CClF_3 . Then from the wealth of dielectric data in $(\text{C}_2\text{F}_6)_{1-x}(\text{CClF}_3)_x$ solid solutions, a phase diagram is constructed. Finally, the reorientation dynamics of $(\text{C}_2\text{F}_6)_{1-x}(\text{CClF}_3)_x$ are analyzed in detail.

II. EXPERIMENTS AND RESULTS

The 99.999% nominal pure chemicals used for this work were mixed in a vessel and condensed into the capacitor which was kept at a constant temperature at around 180 K. The sample temperature was ramped with a constant rate of typically 0.3 K/min. Complex dielectric constants $\epsilon = \epsilon' - i\epsilon''$ were measured using a HP 4274 LCR-meter in the frequency range from 100 Hz to 100 kHz as described previously.^{12,13}

^{a)}Present address: Department of Chemistry, AZ State University, Tempe, Arizona 85287

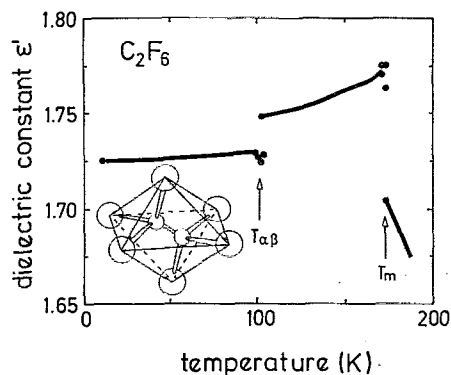


FIG. 1. Dielectric constant of C_2F_6 vs temperature for a measuring frequency of 10 kHz. The fit using the Clausius–Mosotti equation coincides with the liquid state data. A schematic representation of the globular molecular structure of C_2F_6 (taken from Ref. 25) is shown as inset.

A. Dielectric constants

1. Pure C_2F_6

Figure 1 depicts the dielectric constant $\epsilon'(T)$ of the nonpolar compound C_2F_6 in its liquid and solid states. The general shape of the $\epsilon'(T)$ curve resembles that of CCl_4 .¹⁵ Steps in the real part of the dielectric constant document the occurrence of two phase transitions at T_m and $T_{\alpha\beta}$. In the liquid phase the dielectric constant varies linearly with temperature. This type of behavior is characteristic of nonpolar liquids and can well be described by the Clausius–Mosotti equation $P = M/d \times (\epsilon - 1)/(\epsilon + 2)$. The molar polarizability P thus depends on the density d , and the molar mass M . Given $d/\text{gcm}^{-3} = 2.399 - 0.00406 T/\text{K}$ (Ref. 6), the dielectric constants of liquid C_2F_6 shown in Fig. 1 yielded $P = (11.17 \pm 0.01) \text{ cm}^{-3}$. This value is slightly larger than the one for CF_4 .¹⁶ For CF_4 , the polarizabilities just above and just below T_m agree, within experimental errors, indicating that the molecular vibrations giving rise to P are unaffected by melting.¹² This behavior, which seems natural for plastic crystals,¹⁷ is also confirmed for C_2F_6 : from the density of the solid at the melting point $d = 1.85 \text{ gcm}^{-3}$ (Ref. 6), one finds $P = (11.2 \pm 0.1) \text{ cm}^{-3}$, in agreement with the value given above. The determination of the polarizability in the β phase is hampered by the incomplete filling of the sample holder at low temperatures.

2. $(C_2F_6)_{1-x}(CClF_3)_x$ alloys

Figure 2 demonstrates how the dielectric constants of $(C_2F_6)_{1-x}(CClF_3)_x$ interpolate between those of the pure compounds. The Curie law, which describes ϵ' of the liquid state of $CClF_3$ (Ref. 12) is still applicable to the 96% sample, if rescaled to the appropriate dipole concentration x . With steadily decreasing x , $\epsilon'(T)$ reveals three dominant features (Fig. 2): (i) The increase in the dielectric constant seen on cooling which arises from the free rotation of dipoles in the liquid state of $CClF_3$ is reduced and can be separated into two regimes. The regime at lower temperatures, which is considerably flatter and is easily

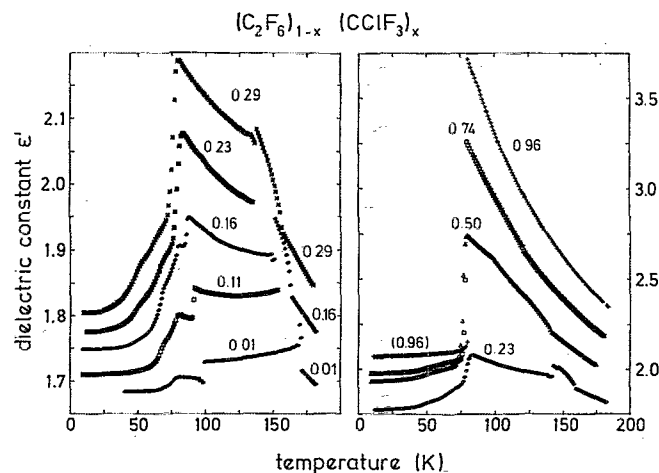


FIG. 2. Dielectric constants $\epsilon'(T)$ of $(C_2F_6)_{1-x}(CClF_3)_x$ alloys at a measuring frequency of 1 kHz. The high temperature data for the samples with $x = 0.11$ and $x = 0.23$ were omitted for clarity.

observed for $x < 0.5$, becomes dominant for low concentrations and finally corresponds to the behavior of $\epsilon'(T)$ in the β phase of C_2F_6 . It thus characterizes a free rotator phase of the solid solutions. (ii) Superimposed on this general behavior are characteristic anomalies which appear in between the two separate regimes of ϵ' . These anomalies collapse into the melting point of pure C_2F_6 . Hence, the region between the two anomalies is interpreted as two-phase coexistence range with the two anomalies marking the liquidus and solidus of the binary system. (iii) A sharp drop in ϵ' ; this drop decreases and broadens upon dilution and is seen only as a gradual change below 23% and finally is almost undetectable for $x < 0.05$.

The large low temperature step in the dielectric constant of the 1% sample at ~ 100 K originates from the $\alpha\beta$ transition as it does for pure C_2F_6 and for higher doping levels. The temperatures at which these steps occur decrease roughly linearly with concentration and for $x \approx 0.23$ merge with the anomalies described above.

In samples with $x < 0.16$, tiny anomalies were detected at $T \approx 79$ K. The origin of these effects is unclear. It is suspected that they might be related to changes in the dynamical behavior of the CF_3 group, since these effects are expected to affect the polarization of the crystals only very slightly. Below temperatures of about 75 K the dielectric constants become frequency dependent, decrease rather smoothly and finally tend to a low-temperature permittivity that roughly scales with x .

B. Dielectric losses

For the whole concentration range, the dielectric losses $\epsilon''(T)$ are presented in Fig. 3. Almost symmetrically shaped loss peaks were detected at low concentrations. Besides a general increase of the amplitudes of the dielectric loss additional features develop at low temperatures as the dipole concentration rises. For purposes of convenience,

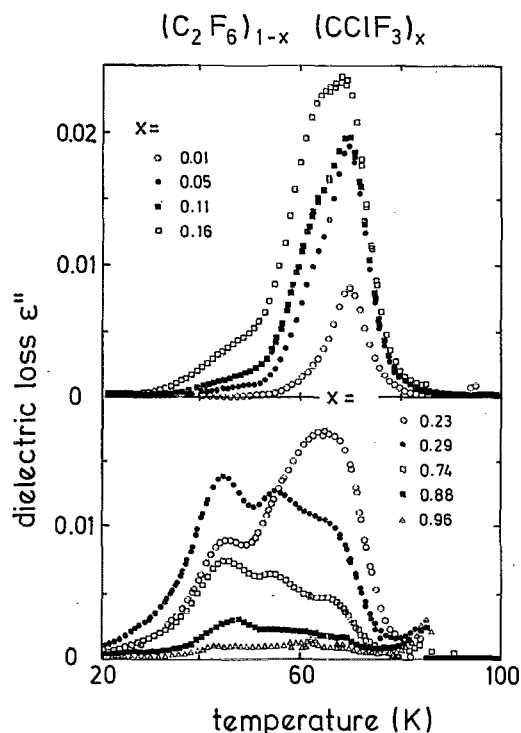


FIG. 3. Temperature dependent dielectric loss of $(\text{C}_2\text{F}_6)_{1-x}(\text{CClF}_3)_x$ measured at a frequency of 1 kHz.

the large high temperature peaks in the upper frame of Fig. 3 will be assigned peak A. For $x = 0.23$ the height of this peak decreases while another one (C) is clearly established (lower frame of Fig. 3). At still larger x , the weight of the peaks changes and intermediate loss maxima show up (peak B). This three peak structure is conserved up to high concentrations, but its amplitude steadily decreases on admixture of CClF_3 and for $x = 0.96$ the dielectric loss $\epsilon''(T)$ is rather small for all T . Such a behavior is expected from a system showing a miscibility gap for $0.25 \lesssim x \lesssim 0.95$, where the height of the dielectric loss scales according to the lever rule.

For concentrations $x > 0.23$ hysteresis effects were observed between 70 and 79 K which pointed towards a first-order phase transition. Taking into account observations from a preliminary X-ray investigation of a $(\text{C}_2\text{F}_6)_{0.5}(\text{CClF}_3)_{0.5}$ sample¹⁸ this effects indicate a transition into a miscibility gap. Remarkably, below $x = 0.23$ no hysteresis is observed. This was taken as a first hint that in this concentration range no phase separation occurs.

As a first step in the evaluation of the dielectric loss data, we plotted the inverse of the temperatures of the loss maxima versus the measuring frequencies ($\log f$). For the maxima of peaks A through C straight lines in this Arrhenius plots were obtained. However, the parameters estimated from the Arrhenius relation

$$\tau = \tau_0 \exp(E/k_B T) \quad (1)$$

have reduced significance since the results presented above imply that $\epsilon''(\log f)$ is symmetric. This assumption is not appropriate for peak A (see Fig. 4) and the same might be

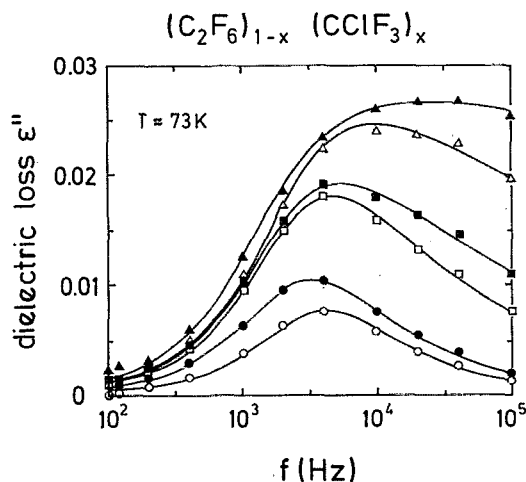


FIG. 4. Dielectric loss $\epsilon''(\omega)$ of $(\text{C}_2\text{F}_6)_{1-x}(\text{CClF}_3)_x$ for different concentrations x : 0.01 (\circ ; $T = 73.1$ K), 0.02 (\bullet ; 72.7 K), 0.05 (\square ; 73.1 K), 0.11 (\blacksquare ; 72.9 K), 0.16 (\triangle ; 73.4 K), and 0.23 (\blacktriangle ; 72.9 K). The solid lines are calculated using Eq. (2). For clarity the dielectric loss of $(\text{C}_2\text{F}_6)_{0.77}(\text{CClF}_3)_{0.23}$ is multiplied by 1.5.

true also for the other peaks. Hence, the quantities for peak B ($\tau_0 = 7 \times 10^{-16}$ s, $E = 1060$ K) and C ($\tau_0 = 5 \times 10^{-15}$ s, $E = 1320$ K) which were evaluated for $x = 0.29$ can be regarded as estimates of the true parameters only. A thorough analysis of the data needs to account for the asymmetric shape of the frequency dependent loss or to deconvolute the dielectric loss spectra in cases where they appear to contain multiple contributions. In Fig. 4 the imaginary part $\epsilon''(\log f)$ of the dielectric constant is shown for various samples with $x \leq 0.23$ at comparable temperatures ($T \approx 73$ K). For a dipole concentration of 1% the loss peak is almost symmetric when plotted versus the logarithm of frequency. It exhibits a full width at half-maximum of about 1.35 decades to be compared with 1.144 for the Debye relaxator. With increasing concentration the half widths taken on the low frequency sides remain constant, the high frequency wing of the distributions flatten and are almost horizontal for $x = 0.23$. The lines in Fig. 4 represent results of fits which will be described in Sec. II B.

III. ANALYSIS AND DISCUSSION

A. Phase diagram

The dielectric technique can be used to detect phase transitions if these couple to discontinuous changes in the polarizability of the specimen. Such abrupt changes can be due to melting or structural transformations as well as order-disorder phenomena. On the other hand, a phase transition is not always detectable by permittivity measurements and the nature of the transition cannot be deduced from the shape of a dielectric anomaly. Keeping these facts in mind, in Fig. 5 the temperatures where the anomalies showed up on cooling were plotted versus the CClF_3 concentration. This procedure did not yield a thermodynamically reasonable phase diagram. One of the simplest ways to put it in compliance with Gibbs' phase rule is the assumption of additional (experimentally unobserved) phase

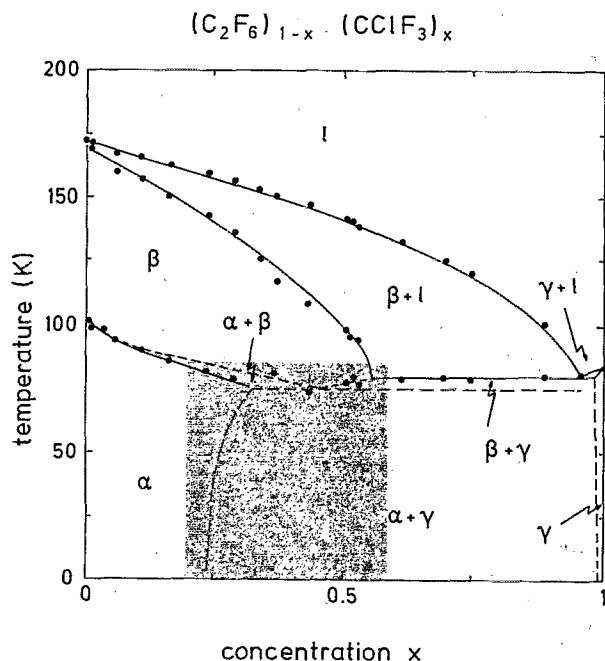


FIG. 5. Phase diagram of $(C_2F_6)_{1-x}(CClF_3)_x$. The lines are drawn to guide the eye. The hatched area indicates the regime where supercooling is easy.

boundaries according to the dashed lines in Fig. 5. In this form, the phase diagram of $(C_2F_6)_{1-x}(CClF_3)_x$ exhibits two eutectic points. The one involving the liquid solution is located at $0.96 < x < 1$. The phase equilibria near the other eutectic point at $0.3 \lesssim x \lesssim 0.5$ involve solid phases only. This explains why supercooling is easily achieved at these concentrations.³ Remarkable features of the phase diagram are the large hysteresis of the $\alpha\beta$ boundary (on heating the transformation back to the β phase is complete only at $T = (104 - 20x)K$ and the huge width of the regimes where mixed crystals with the ordered (α) and disordered (β) modifications of solid C_2F_6 show up. The latter observation is compatible with results from preliminary x-ray investigation on a $(C_2F_6)_{0.5}(CClF_3)_{0.5}$ sample.¹⁸ The extension of the α phase up to concentrations of $x \approx 0.25$ is obvious from the results of the following analysis of the dielectric losses.

B. Dipolar relaxation

In certain composition ranges, the temperatures dependent dielectric loss spectra share typical features: At low concentrations with $x \lesssim 0.16$, a one peak structure is found which passes over to a pattern that is built up from several distinguishable peaks at larger x . Finally, within the miscibility gap ($0.25 \lesssim x \lesssim 0.98$), only the amplitudes of the $\epsilon''(\omega)$ spectra vary with concentration. In the following, the behavior within the different composition regimes will be interpreted qualitatively. Then a quantitative analysis of the high temperature dielectric losses ($T \gtrsim 65$ K) of samples with $x < 0.23$ will be presented.

For $x < 0.16$ one dominant peak (A) appears in Fig. 3. Obviously, at these low concentrations, crystal field effects

dominate and the dipolar interactions are weak and almost negligible. Thus, a tagged $CClF_3$ dipole essentially probes the hindering barriers of the crystal field of the nonpolar C_2F_6 host. At lower temperatures relatively small additional contributions increase with the concentration x , i.e., with the successive substitution of neighboring C_2F_6 molecules by the smaller $CClF_3$ dipoles. For the tagged $CClF_3$ relaxators, this provides additional reorientation paths. Due to the size effect, the steric hindrance along these paths is smaller, and the corresponding energy barrier is lower. This naturally gives rise to dielectric loss contributions on the low-temperature wing of the peaks in the upper frame of Fig. 3.

For dipole concentrations of 20%, the most probable environment of a tagged $CClF_3$ molecule is that with five nonpolar and one dipolar molecules in the surrounding shell. (Calculated from the binominal distribution for a six-fold⁹ coordinated lattice.) But there is a considerable amount ($> 30\%$) of $CClF_3$ relaxators with more than one adjacent small molecule. Therefore it is not surprising that with increasing concentrations the weight of the dielectric loss peaks change in favor of the low barrier processes. Finally, within the miscibility gap, all the C_2F_6 -rich crystallites are expected to have a concentration which is given by the $(\alpha, \alpha + \gamma)$ coexistence curve. Thus only the amplitude of the $\epsilon''(T)$ pattern changes as explained in Sec. II B.

Similar observations can be made from the frequency dependent dielectric loss curves. At low concentrations x , only one $\epsilon''(\omega)$ peak is resolved at audio frequencies. For samples with $x > 0.29$ several loss peaks show up in the ϵ'' vs T spectra. However, already for $x < 0.29$ the increasing contributions from low barrier processes are clearly established and lead to additional high-frequency absorptions (Fig. 4). The $\epsilon''(\omega)$ spectra can be thought to be composed from several reorientation processes and an analysis of the experimental results in terms of a sum of several different relaxators is certainly possible. However, the number of adjustable parameters required for such a description is comparable to the number of measured frequencies. Therefore we tried to find a reasonable parametrization of the data from which significant physical parameters such as the static dielectric susceptibilities χ_s and the relaxation times τ could be determined.

Several well-known expressions to model dielectric loss spectra were attempted, among them the formulas by Cole and Cole,¹⁹ by Williams and Watts,²⁰ or by Cole and Davidson.²¹ All of them gave a good fit for certain concentrations. This is demonstrated in Fig. 6 for the frequency-dependent dielectric loss of the crystals with $x = 0.01$ and 0.05 and in Fig. 7 for the temperature dependent losses of $(C_2F_6)_{0.98}(CClF_3)_{0.02}$. However, only the Cole-Davidson function provided a satisfactory parametrization for all concentrations x . The imaginary part of the Cole-Davidson expression reads

$$\epsilon'' = 4\pi\chi_s(\cos\varphi)^\beta \sin(\beta\varphi), \quad (2)$$

and $\varphi = \text{atan}(2\pi f\tau)$. The parameter β is a measure for the deviations from Debye behavior ($\beta = 1$). The Debye

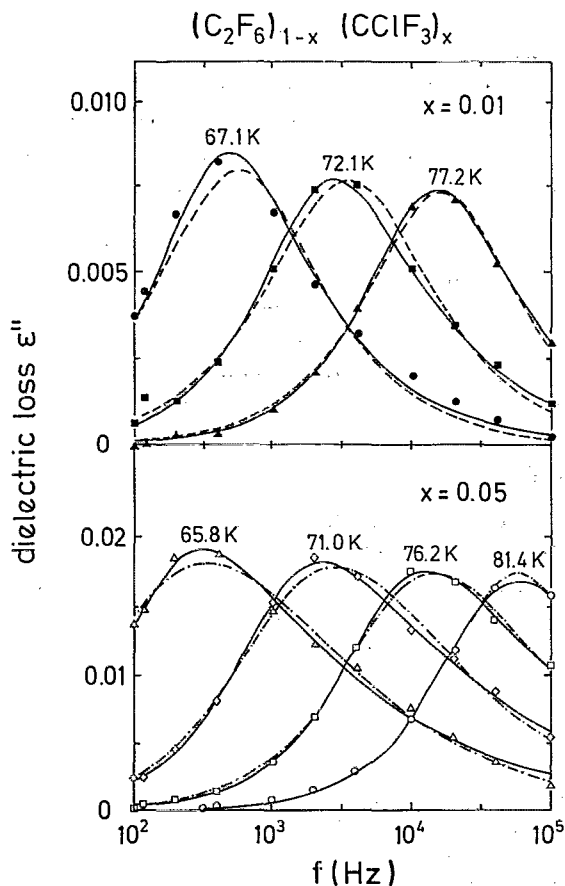


FIG. 6. Fits with various functions to the dielectric loss of $(\text{C}_2\text{F}_6)_{1-x}(\text{CClF}_3)_x$. The temperatures are indicated. For two concentrations the experimental results are compared with the results of different fits: Upper frame, $x = 0.01$ and lower frame, $x = 0.05$. The solid lines are calculated using Eq. (2). Dashed lines were computed with the Cole-Cole expression and the width parameter $\alpha \approx 0.1$. Fits with a Williams-Watts function and an exponent of approximately 0.55 are represented by the dash-dotted lines.

model applies to dielectrics that can be characterized by a single relaxation time. The 1% sample is close to this ideal behavior since the CClF_3 probes are located in an almost homogeneous nonpolar C_2F_6 environment. Hence, β is relatively close to unity (Fig. 8). On the other hand, in $(\text{C}_2\text{F}_6)_{0.77}(\text{CClF}_3)_{0.23}$, the parameter β is vanishingly small and indicates the presence of several relaxation mechanisms.

The relaxation times from the fits obeyed Arrhenius laws [Eq. (1)] with prefactors $\tau_0 = 1.7 \times 10^{-15}$ s. Also the energy barriers $E = (1785 \pm 30)$ K are almost constant for $x < 0.23$. The difference between the barriers of the 1% and the 23% samples is 60 K which is much smaller than the concentration dependence of E in $(\text{CF}_4)_{1-x}(\text{CClF}_3)_x$ which increased from ~ 1500 K in CF_4 to ~ 1700 K on adding only 1.1% of CClF_3 .¹³ By comparison with the present alloys, it can be concluded that this latter increase is due to a considerable distortion of the CF_4 host and not due to electric interactions between the CClF_3 dipoles. Dipolar interaction forces would result in a concentration dependence of the hindering barriers in

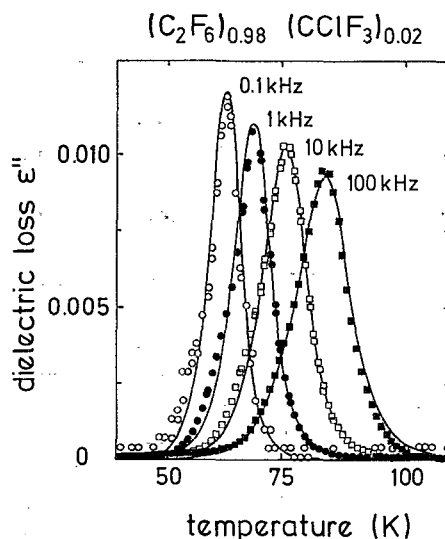


FIG. 7. Temperature dependence of the dielectric loss of $(\text{C}_2\text{F}_6)_{1-x}(\text{CClF}_3)_x$ for different measuring frequencies. The solid lines were calculated using the parameters $C = 6.3$ K, $\beta = 0.61$, $\tau_0 = 1.52 \times 10^{-15}$ s, and $E = 1785$ K.

$(\text{CF}_4)_{1-x}(\text{CClF}_3)_x$ as well. Obviously the large strain fields are driving the unmixing of $(\text{CF}_4)_{1-x}(\text{CClF}_3)_x$ at dipole concentrations in excess of 1.5%.¹³ Solution theories predict that the miscibility of CClF_3 in C_2F_6 should be better than in CF_4 , since it is generally much easier to dissolve a small molecule in the lattice of a large one than vice versa.²² In $(\alpha\text{-C}_2\text{F}_6)_{1-x}(\text{CClF}_3)_x$ formation of mixed crystals is observed up to $x \approx 0.25$. This will be demonstrated in the following.

The integrated area under the loss curves plotted on a logarithmic frequency scale is a measure of the static susceptibility which should be proportional to the number of

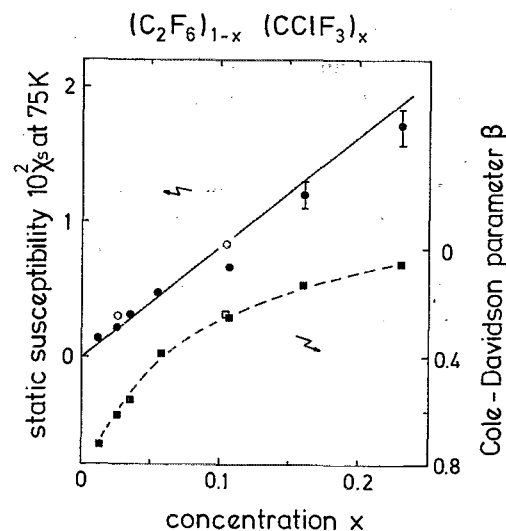


FIG. 8. Mean static susceptibility χ_s (variations represented as bars) and Cole-Davidson parameter β from fits to data of slowly cooled (full symbols) and quenched samples (open symbols). The solid line is calculated with the Curie law $\chi_s = xC/T$ with $C = 6$ K at $T = 75$ K.

dipoles in the sample as long as no unmixing takes place. The static susceptibilities of several slowly cooled $(\text{C}_2\text{F}_6)_{1-x}(\text{CClF}_3)_x$ crystals and two quenched samples²³ with $x = 0.02$ and $x = 0.10$ were deduced from fits for temperatures $65 \text{ K} < T < 85 \text{ K}$. For all concentrations χ_s increased slightly with decreasing temperatures. Figure 8 reveals that the mean susceptibilities (measured at 75 K) increase almost linearly with concentration.

The discussion of the relaxation times suggests that the CClF_3 molecules relax almost independent from each other. For these paraelectric processes one finds $\chi_s = xC/T$ with the Curie constant $C = n_0 p^2 / 3k_B$. The number density $n_0 = 1.24 \times 10^{22} \text{ cm}^{-3}$ was estimated from the density $d = 2.06 \text{ g/cm}^3$ of C_2F_6 at 90 K.⁹ Taking $p = 0.5 \text{ D}$ for the dipole moment from the measurements of the gas phase of CClF_3 (Ref. 24), one arrives at $C = 7.5 \text{ K}$. This value compares excellently with the mean value $C_{\text{ex}} = 6 \text{ K}$ used to fit the dielectric data up to $x = 0.23$ (Fig. 7). Besides the general difficulties, when evaluating Curie constants¹³ another problem is evidenced in Fig. 3: The relaxation process at 75 K does not slow down every dipole, which is inferred from additional absorption processes which occur at lower temperatures. These contributions become more important at high concentrations and lead to increasing deviations from the solid line in Fig. 8.

IV. SUMMARY AND CONCLUSIONS

In this paper we have studied slowly cooled $(\text{C}_2\text{F}_6)_{1-x}(\text{CClF}_3)_x$ alloys in their solid and liquid phases. For pure C_2F_6 , the molar polarizabilities were calculated from the dielectric constants. A phase diagram was constructed which involves two eutectic points. The phase diagram exhibits solid-state miscibility up to dipole concentrations of $x > 0.5$ at high temperatures. This β phase (Fig. 5) is orientationally disordered with fast reorientations of the CClF_3 dipoles. It is this regime which is susceptible to supercooling which will be demonstrated in the succeeding paper.³ At low temperatures $(\alpha\text{-C}_2\text{F}_6)_{1-x}(\text{CClF}_3)_x$, thermally equilibrated mixed crystals can be obtained up to $x \approx 0.25$. The relaxation dynamics of these samples were studied in detail. The data analysis accounted for the static susceptibility of the solid solutions as well as of the shape of their dielectric loss curves.

The results are the following: at low concentrations, the $\epsilon''(\log f)$ loss spectra are symmetrically shaped and the CClF_3 dipoles probe the crystal field which is produced by adjacent C_2F_6 molecules. As the concentration increases, relaxation channels with lower effective energy

barriers become available. This leads to additional contributions to the dielectric loss at low temperatures (Fig. 3) or high frequencies (Fig. 4). For samples with dipole concentrations $x > 0.2$, the increasing inhomogeneities of the crystals fields are reflected by the appearance of an increasing number of relaxation peaks. Finally, at $x \lesssim 0.25$, the alloys segregate.

Usually, in mixed crystals with such a large range of miscibility, the dipolar interactions lead to a complete smearing out of the relaxation spectra.¹ On the other hand, in $(\text{C}_2\text{F}_6)_{1-x}(\text{CClF}_3)_x$ the random fields are mainly produced by the different sizes of the constituent molecules which give rise to only locally disturbed crystal fields.

ACKNOWLEDGMENTS

We thank L. Gruber, H. Klee, and K. Knorr for making results from their unpublished x-ray experiments available. This work was supported by the Sonderforschungsbereich 262 and by the Materialwissenschaftliches Forschungszentrum Materials Science Research Center Mainz.

¹U. T. Höchli, K. Knorr, and A. Loidl, *Adv. Phys.* (1990), in press; A. Loidl, *Annu. Rev. Phys. Chem.* **40**, 20 (1989).

²K. Binder and A. P. Young, *Rev. Mod. Phys.* **58**, 801 (1986).

³R. Böhmer and A. Loidl, *J. Chem. Phys.* (to be published).

⁴N. G. Parsonage and L. A. K. Staveley, *Disordered in Crystals* (Clarendon, Oxford, 1978).

⁵E. L. Pace and J. G. Aston, *J. Am. Chem. Soc.* **70**, 566 (1948).

⁶O. Ruff and O. Brettschneider, *Z. Anorg. u. Allg. Chem.* **210**, 173 (1933).

⁷H. S. Gutowsky and G. E. Pake, *J. Chem. Phys.* **18**, 162 (1950); see also H. S. Gutowsky, G. B. Kistiakowsky, G. E. Pake, and E. M. Purcell, *ibid.* **17**, 972 (1949).

⁸J. H. Smith and E. L. Pace, *J. Phys. Chem.* **73**, 2368 (1969).

⁹A. Lewis and E. L. Pace, *J. Chem. Phys.* **58**, 3661 (1973).

¹⁰G. S. Pawley and A. W. Hewat, *Acta Crystallogr. B* **41**, 136 (1985).

¹¹R. C. Miller and C. P. Smyth, *J. Am. Chem. Soc.* **79**, 20 (1957).

¹²R. Böhmer and A. Loidl, *J. Chem. Phys.* **89**, 4981 (1988).

¹³R. Böhmer, *J. Chem. Phys.* **91**, 3111 (1989).

¹⁴D. van der Putten, F. Fujara, and R. Böhmer (to be published).

¹⁵A. Di Giacomo and C. P. Smyth, *J. Am. Chem. Soc.* **78**, 2032 (1956).

¹⁶P. Tremaine and R. G. Robinson, *Can. J. Chem.* **51**, 1497 (1970).

¹⁷R. Böhmer and A. Loidl, *Z. Phys. B-Condensed Matter* **80**, 139 (1990).

¹⁸L. Gruber, H. Klee, and K. Knorr (unpublished).

¹⁹K. S. Cole and R. H. Cole, *J. Chem. Phys.* **9**, 341 (1941).

²⁰G. Williams and D. C. Watts, *Trans. Faraday Soc.* **66**, 80 (1970).

²¹D. W. Davidson and R. H. Cole, *J. Chem. Phys.* **19**, 1484 (1951).

²²J. H. Hildebrand and R. L. Scott, *The Solubility of Nonelectrolytes*, 3rd ed. (Reinhold, New York, 1950), p. 304.

²³These samples were supercooled from the β phase according to the experimental procedure described in Ref. 3.

²⁴H. Sutter and R. H. Cole, *J. Chem. Phys.* **52**, 132 (1970).